Dynamics of HIV Infection: A Cellular Automata Approach

Rita Maria Zorzenon dos Santos*
Instituto de Física de São Carlos, Universidade de SãoPaulo, CP 369, CEP 13560-970, São Carlos, São Paulo, Brazil

Sérgio Coutinho†
Laboratório de Física Teórica e Computacional, Universidade Federal de Pernambuco, CEP 50670-901, Recife, Pernambuco, Brazil
(Received 31 July 2000; published 26 September 2001)

We use a cellular automata model to study the evolution of human immunodeficiency virus (HIV) infection and the onset of acquired innumodeficiency syndrome (AIDS). The model takes into account the global features of the immune response to any pathogen, the fast mutation rate of the HIV, and a fair amount of spatial localization, which may occur in the lymph nodes. Our results reproduce the three-phase pattern observed in T cell and virus counts of infected patients, namely, the primary response, the clinical latency period, and the onset of AIDS. The dynamics of real experimental data is related to the transient behavior of our model and not to its steady state. We have also found that the infected cells organize themselves into spatial structures, which are responsible for the decrease on the concentration of uninfected cells, leading to AIDS.

DOI: 10.1103/PhysRevLett.87.168102 PACS numbers: 87.18.Hf, 02.70.–c, 87.15.Aa, 87.19.Xx

In the last decades the infection by the human immunodeficiency virus (HIV), which causes AIDS (acquired immunodeficiency syndrome), has been the subject of most intense studies that encompass diverse fields of scientific research. Although major progress has been achieved by medical and biological researchers in understanding different aspects of the virus-host interaction, the mechanisms by which HIV causes AIDS still remain unexplained.

The immune response to any virus is generated by a complex web of interactions among different types of white blood cells (monocytes, T and B cells). The time scale to develop a specific immune response may vary from days to weeks. In the case of HIV, the entire course of infection involves two different time scales [1]. The primary infection exhibits the same characteristics as any other viral infection: a dramatic increase of the virus population during the first 2–6 weeks, followed by a sharp decline, due to the action of the immune system. However, instead of being completely eliminated after the primary infection, as many other viruses, a low HIV concentration is detected for a long asymptomatic time: the clinical latency period. This period may vary from one to ten (or more) years. Besides the low virus burden detected during this period, a gradual deterioration of the immune system is manifested by the reduction of $CD4^+$T-cell populations in the peripheral blood. The third phase of the disease is achieved when the concentration of the T cells is lower than a critical value ($\sim$30%), leading to the development of AIDS. As a consequence, the patient normally dies from opportunistic diseases. This common pattern observed in infected patients [1] is depicted in Fig. 1, which shows the plasma viremia titer and the $CD4^+$T cell counts in the peripheral blood as functions of time.

Several theories [2] have been proposed to explain why and how the virus remains in the organism after the primary immune response, and the causes of the decline of T-cell counts, leading to the onset of AIDS. So far, none of them has provided a complete explanation for the entire process.

Mathematical models have also been developed to try to understand the dynamics of the HIV infection. Most of them use ordinary (or partial) differential equations to describe different aspects of the dynamics of the host-parasite interaction (for a review see [3]). Although many of them have contributed to the understanding of various aspects of the development of the disease, they fail to describe the two time scales observed in the course of infection: the short time scale (few weeks) associated with the primary response and the long one (few years) associated with the clinical latency period and the onset of AIDS. These mean-field-like models do not take into account the local interactions and the spatial inhomogeneities, caused by localization of the initial immune response in the lymphoid organs. We believe that these features, which are natural ingredients of our model, are of central importance. From the dynamical point of view, these different time scales may be related to two kinds of interactions: one local and fast, and the other long-ranged and slow.

Experimental evidence [4] supports that the lymph nodes are major reservoirs of HIV infection *in vivo*. A snapshot of the distribution of cells among the different compartments of the immune system will show only a small fraction (2%–4%) of the cells circulating in blood and lymph, while the majority is found in the lymphoid organs [5]. Paradoxically, the process of mobilization and activation of immune cells directed against the virus that occurs in the lymphoid micro-environment, in the case of the HIV, provides a milieu that contributes to the virus spread [4].

Recently, one of us has shown that cellular automata models may describe well experimental patterns observed in immune responses [6]. Since this kind of approach

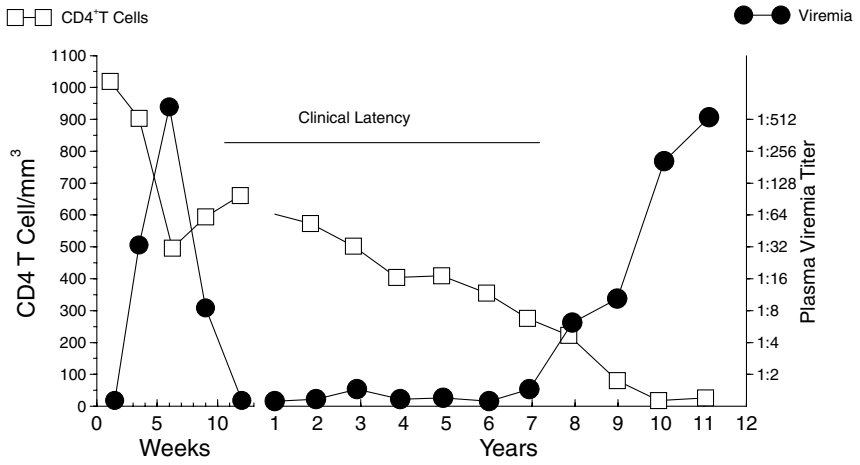

FIG. 1. The common pattern exhibited by infected patients, first presented by Pantaleo *et al.* [1]. The plasma viremia titer (black circles) and CD4$^+$T cell counts (squares) versus time show a three-phase dynamics.

is suitable to describe the local interactions, we use it to model the course of the HIV infection. We assume that the HIV infection does not affect substantially the overall behavior of the immune system [7]. Our model tests whether the combination of a healthy immune system with the high mutation rate of the HIV and a fair amount of spatial localization, occurring in the lymphoid tissues, may explain the three-phase dynamics observed during the course of the infection (see Fig. 1). The results obtained from simulations of our model are shown in Fig. 2, and as far as we know, this is the first time that the entire course of the HIV infection process is so faithfully reproduced by a theoretical model, without any change of the parameter set during the simulations.

A lymph node has a mesh structure with different sites of interactions that may be approximated by a rough surface [8]. Therefore we model the interaction among the immune system cells in the lymphoid tissues using a square lattice. With each site we associate a cell that may be a CD4+T cell or a monocyte that is the main target for the HIV [1]. The four-state automaton corresponds to the states of the cell, which may be found in these tissues to mount the immune response. Each cell can be in one of following states: (a) *healthy;* (b) *infected-A1,* corresponding to an infected cell that is free to spread the infection; (c) *infected-A2,* the final stage of an infected cell before it dies due to the action of the immune system; and, finally, (d) *dead,* an infected cell that was killed by the immune response.

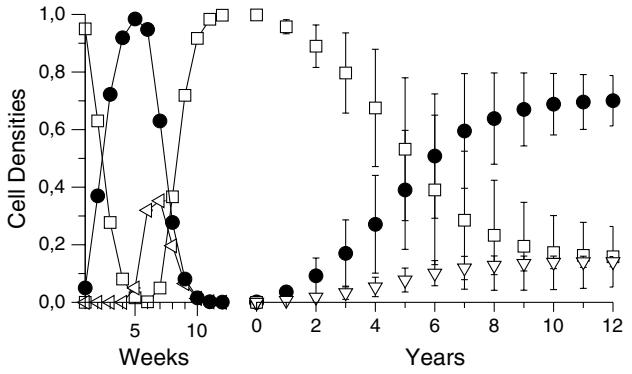

FIG. 2. The results obtained from our simulations for a two-dimensional lattice with $L = 700$, $p_{\mathrm{HIV}} = 0.05$, $R = 4$, $\tau = 4$, $p_{\mathrm{infec}} = 10^{-5}$, $p_{\mathrm{repl}} = 0.99$. The evolution of the population densities exhibits the same three-phase dynamics observed for infected patients. We have adopted *open squares* for healthy cells, *full circles* for infected cells, and *open triangles* for dead cells.

The initial configuration is composed of healthy cells, with a small fraction, p_{HIV}, of infected-A1 cells, representing the initial contamination by the HIV. In one time step the entire lattice is updated in a synchronized parallel way, according to the rules described below. The updated state of a cell depends on the states of its four nearest neighbors and the four next nearest neighbors, in a square lattice.

Rule 1: Update of a healthy cell: (a) If it has at least one infected-A1 neighbor, it becomes infected-A1. (b) If it has no infected-A1 neighbor but does have at least R ($2 < R < 8$*) infected-A2 neighbors, it becomes infected-A1. (c) Otherwise it stays healthy.*—Rule 1a mimics the spread of the HIV infection by contact, before the immune system had developed its specific response against the virus. Rule 1b represents the fact that infected-A2 cells may, before dying, contaminate a healthy cell if their concentration is above some threshold.

Rule 2: An infected-A1 cell becomes infected-A2 after τ *time steps.*—An infected-A2 cell is the one against which the immune response has developed, and hence its ability to spread the infection is reduced. Here τ represents the time required for the immune system to develop a specific response to kill an infected cell. Such a time delay is required for each infected cell since in our model we view each new infected cell as carrying a different lineage (strain) of the virus. This is the way we incorporate the mutation rate of the virus in our model. When a healthy cell is infected, the virus uses the cell's DNA in order to transcribe its RNA and replicate. During each transcription an error may occur, producing, on the average, one

mutation per generation and hence a new strain of the virus is produced [9,10].

Rule 3: Infected-A2 cells become dead cells.—This rule simulates the depletion of the infected cells by the immune response.

Rule 4: (a) Dead cells can be replaced by healthy cells with probability p_{repl} in the next time step (or remain dead with probability $1 - p_{\mathrm{repl}}$). (b) Each new healthy cell introduced may be replaced by an infected-A1 with probability p_{infec}.—Rule 4a describes the replenishment of the depleted cells, mimicking the high ability of the immune system to recover from the immunosuppression generated by infection. As a consequence, it will also mimic some diffusion of the cells in the tissue. Rule 4b simulates the introduction of new infected cells in the system, either coming from other compartments of the immune system or resulting from the activation of the latent infected cells, as suggested in the literature.

We performed simulations of the model, using periodic boundary conditions, on a lattice of $N = L^2$ sites with L ranging from 300 up to 1000. All the adopted parameters were based on experimental data: $p_{\mathrm{HIV}} = 0.05$ was chosen based on the observation that one in 10^2 or 10^3 T cells harbor viral DNA during the primary infection [11]; $p_{\mathrm{infec}} = 10^{-5}$ is due to the fact that only one in 10^4 to 10^5 cells in the peripheral blood of infected individual expresses viral proteins; to simulate the high ability of the immune system to replenish the depleted cells, we used $p_{\mathrm{repl}} = 0.99$, although smaller probabilities could also be considered; since the delay parameter (τ) may vary from 2 to 6 weeks, we chose $\tau = 4$. Each of our time steps corresponds to one week.

In Fig. 2, we present the evolution of the densities of healthy cells, infected cells (A1 and A2 types), and dead cells, obtained from simulations of our model. We show the results averaged over 500 simulations and the corresponding standard deviations (error bars). Each sample corresponds to different initial configurations and therefore different individuals. There is qualitative agreement between our results for the density of healthy and infected cells and the time evolution of the number of CD4+ T cells in the peripheral blood and the plasma viremia titer shown in Fig. 1. The model reproduces the two time scales observed in the dynamics of the HIV infection. The small error bars at the primary infection indicate that its dynamics is insensitive to the initial configuration, in contrast to what occurs in the latency period.

Our model allows a closer look at local behavior. From the analysis of the spatial configurations randomly generated by the model in individual simulations, we noticed that the slow dynamics and the large deviations, observed in the latency period, are related to the emergence, after completion of the primary response, of some spatial structures of infected cells. These growing special structures spread the infection in such a way that they slowly commit more and more healthy cells, segregating and trapping uninfected cells.

In Fig. 3 we present four "snapshots" of typical configurations obtained during one particular simulation. Starting from an initial configuration composed of healthy cells (blue) with a random distribution of infected-A1 cells (yellow), in the subsequent time steps each individual infected-A1 cell generates a pulse of infected cells, of width $(\tau + 1)$, propagating in all directions. Whenever the average distance $\langle l_1 \rangle$ between individual infected cells in the initial configuration is less than or equal to $(2\tau + 1)$, the independent pulses achieve a maximum coverage of the lattice. For $\tau = 4$ the maximum coverage occurs after five weeks as shown in Fig. 3a. After that the concentration of infected cells decreases to a minimal value at $2(\tau + 1)$ time steps, establishing the end of the primary infection phase (10 weeks, in this case).

In the following time steps the presence of infected cells will be dictated by $p_{\mathrm{newinfec}} = p_{\mathrm{repl}} * p_{\mathrm{infec}}$, according to rule 4. When new infected cells are introduced, they may generate two different kinds of structures. The simplest one corresponds to a wave of infected cells propagating in all directions. But in this case, since $p_{\mathrm{newinfec}} \ll p_{\mathrm{HIV}}$ the average distance $\langle l_2 \rangle$ between the new infected cells, introduced at random locations, is much larger than $(2\tau + 1)$. The spread of infection generated only by these structures takes a longer time to cover the lattice, and after that the infection vanishes. It is very rare, however, to find only these simple structures. Examples of such structures are shown in the bottom right of Figs. 3b and 3c. A second type of structure also occurs, due to the interplay between

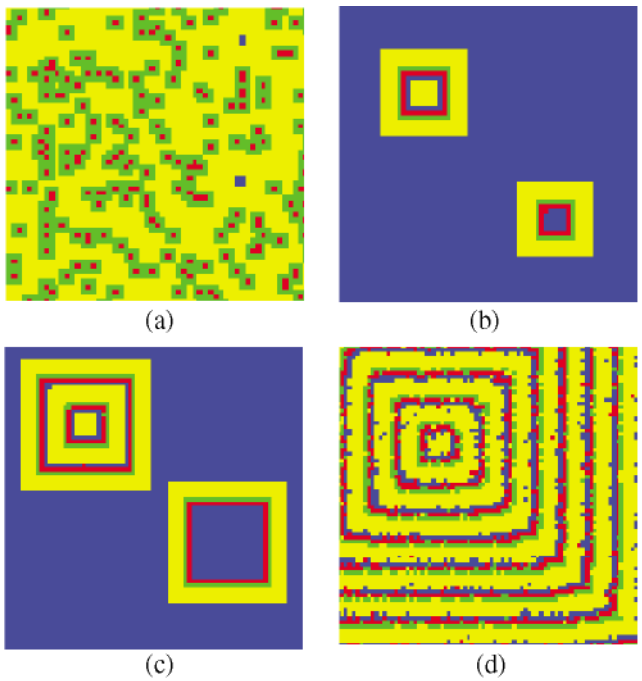

FIG. 3 (color). Four snapshots of parts of the lattice configuration for different time steps: (a)–(d) correspond to 5, 18, 25, and 200 weeks, respectively. We have adopted the same parameters used in Fig. 2. The color codes for the different states of the cell are the following: healthy=blue, infected-A1=yellow, infected-A2=green, and dead=red.

rules 1b, 4a, and 4b. These special structures are generated by "sources" of infected cells. These sources appear, for instance, when a new infected-A1 cell, introduced by rules 4a and 4b, is surrounded by at least R dead cells ($R = 4$ for the results shown here). At every $(\tau + 3)$ time steps they launch a propagating wave front of infected cells with width $(\tau + 1)$. Figures 3b and 3c (upper left) show such structures for two subsequent periods, corresponding, respectively, to 18 and 25 weeks. As these structures grow, the number of infected cells increases and the concentration of healthy cells decreases, as observed in infected patients during the latency period. These growing structures may eventually cover the entire lattice, with the densities of cells evolving towards steady states. Note that the final average density of healthy cells is always below the threshold of the $CD4_+$ T cells counts, which is related to the onset of AIDS. Therefore according to our findings, the dynamics of real experimental data, shown in Fig. 1, would correspond to the transient behavior of our model.

Analysis of the source distribution at any given time shows that the latency period depends on $\langle l_3 \rangle$, the average distance between sources and, consequently, on the probability of occurrence of such sources. Actually, since new sources can be released at any time step, the length of the transient time depends on the spatiotemporal average of the distance between the sources. These growing structures of infected cells may be associated with syncytia, an aggregation of infected cells observed experimentally, and according to our results they would be responsible for the depletion of T cells leading to AIDS. These results actually corroborate some previous suggestions that syncytia could be responsible for the permanence of the virus in the system, based on the analysis of the similarities between HIV infection and other diseases [2,12].

In this work we have shown that our cellular automaton model reproduces quite well the three-stage dynamics (two time scales) of the HIV infection, as observed in the infected patients, without changing the parameter set during the simulation. The short time scale, characteristic of the primary infection, increases when τ is increased or when p_{HIV} decreases. The long time scale, responsible for the clinical latency period and the onset of AIDS, is associated with the emergence of sources of infected cells and the formation of special structures that slowly increase the number of infected cells and confine healthy cells. This special pattern formation depends on the value of the parameter R of rule 1b, p_{repl}, and p_{infec}. Our results indicate that in contrast to the ordinary differential equation models, the clinical latency does not correspond to a steady state but to a long transient. The reason for our success in describing the three-stage dynamics, whereas the other approaches fail, is that we take into account local interactions, which may occur in the lymph nodes, that play a major role on the course of the infection. Our findings corroborate the importance of the lymph nodes, the spatial localization, and the local interactions on the dynamics of HIV infection, as suggested in the medical literature [4].

We found that these results are reproducible for a wide range of the parameters. The complete study of the parameter space, the detailed discussion of the necessary conditions to generate the special structures, and the role they play spreading the infection will be published elsewhere.

This work and another one [13] published after submission of our manuscript further substantiate claims made in previous studies [6] that discrete models may be useful to describe emergent properties of complex biological systems, and to understand the mechanisms underlying its dynamical behavior.

Finally, it is worth mentioning the work of Mannion and collaborators [14], who use stochastic discrete models to study some aspects related to the dynamics of HIV infection.

We thank Dr. M. Curié Cabral, I. Procaccia, S. Bocalletti, and J-P. Eckmann for enlightening discussions and to Borko Stošic for assistance with color graphics. R. M. Z. S. thanks J. F. Fontanari for the hospitality during her visit to IFSC-USP, and FAPESP (Project No. 99/09999-1) for supporting her stay. This work was partially supported by the Brazilian Agencies CNPq, CAPES, FINEP (under Grant No. PRONEX 94.76.0004/97), and FAPERJ.

*Permanent address: Instituto de Física, Universidade Federal Fluminense, Av. Litorânea s/n- CEP 24210-340, Niterói, Rio de Janeiro, Brazil.
Email address: zorzenon@if.uff.br
†Email address: sergio@lftc.ufpe.br

[1] G. Pantaleo, C. Graziozi, and A. S. Fauci, New England J. Med. **328**, 327 (1993).
[2] A. S. Fauci, Science **239**, 617 (1988).
[3] A. S. Perelson and P. W. Nelson, SIAM Rev. **41**, 3 (1999), and references therein.
[4] O. J. Cohen, G. Pantaleo, G. K. Lam, and A. S. Fauci, Springer Semin. Immunopathol. **18**, 305 (1997).
[5] D. J. Steckel, J. Theor. Biol. **186**, 491 (1997); D. J. Steckel *et al.,* Immunol. Today **18**, 216 (1997).
[6] R. M. Zorzenon dos Santos and A. T. Bernardes, Phys. Rev. Lett. **81**, 3034 (1998); R. M. Zorzenon dos Santos, in *Annual Reviews of Computational Physics,* edited by D. Stauffer (World Scientific, Singapore, 1999), Vol. VI, pp. 159–202.
[7] D. D. Ho *et al.,* Nature (London) **373**, 123 (1995).
[8] L. E. Hood, I. L. Weissmann, W. B. Wood, and J. H. Wilson, *Immunology* (The Benjamin/Cummings Publishing Company, Menlo Park, CA, 1984), 2nd ed.
[9] M. A. Nowak and A. J. Michael, Sci. Am. **273**, No. 2, 42 (1995).
[10] W. C. Drosopoulos *et al.,* J. Mol. Med. (Berlin) **76**, 604 (1998).
[11] S. M. Schnittman *et al.,* Science **245**, 305 (1998); S. M. Schnittman *et al.,* Ann. Intern. Med. **113**, 438 (1990).
[12] R. A. Weiss, Science **272**, 1885 (1996).
[13] U. Hershberg, Y. Louzoun, H. Athan, and S. Solomon, Physica (Amsterdam) **289A**, 178 (2001).
[14] R. Mannion, H. Ruskin, and R. B. Pandey, Theor. Biosc. **119**, 10 (2000); **119**, 94 (2000).